land

MDPI

Article

Prediction Modeling and Driving Factor Analysis of Spatial Distribution of CO_2 Emissions from Urban Land in the Yangtze River Economic Belt, China

Chao Wang [1,2,3,*], Jianing Wang [1], Le Ma [1], Mingming Jia [4], Jiaying Chen [5], Zhenfeng Shao [1] and Nengcheng Chen [1,3]

1 State Key Laboratory of Information Engineering in Surveying, Mapping and Remote Sensing, Wuhan University, Wuhan 430079, China; jianing.w@whu.edu.cn (J.W.); malele@whu.edu.cn (L.M.); shaozhenfeng@whu.edu.cn (Z.S.); chennengcheng@cug.edu.cn (N.C.)
2 Key Laboratory of Basin Water Resources and Eco-Environmental Science in Hubei Province, Changjiang River Scientific Research Institute of Changjiang Water Resources Commission, Wuhan 430010, China
3 National Engineering Research Center of Geographic Information System, School of Geography and Information Engineering, China University of Geosciences (Wuhan), Wuhan 430074, China
4 State Key Laboratory of Black Soils Conservation and Utilization, Northeast Institute of Geography and Agroecology, Chinese Academy of Sciences, Changchun 130102, China; jiamingming@iga.ac.cn
5 College of Resources and Environment, Huazhong Agricultural University, Wuhan 430070, China; chen.jiaying@mail.hzau.edu.cn
* Correspondence: c.wang@whu.edu.cn

Abstract: In recent years, China's urbanization has accelerated, significantly impacting ecosystems and the carbon balance due to changes in urban land use. The spatial patterns of CO_2 emissions from urban land are essential for devising strategies to mitigate emissions, particularly in predicting future spatial distributions that guide urban development. Based on socioeconomic grid data, such as nighttime lights and the population, this study proposes a spatial prediction method for CO_2 emissions from urban land using a Long Short-Term Memory (LSTM) model with added fully connected layers. Additionally, the geographical detector method was applied to identify the factors driving the increase in CO_2 emissions due to urban land expansion. The results show that socioeconomic grid data can effectively predict the spatial distribution of CO_2 emissions. In the Yangtze River Economic Belt (YREB), emissions from urban land are projected to rise by 116.23% from 2020 to 2030. The analysis of driving factors indicates that economic development and population density significantly influence the increase in CO_2 emissions due to urban land expansion. In downstream cities, CO_2 emissions are influenced by both population density and economic development, whereas in midstream and upstream city clusters, they are primarily driven by economic development. Furthermore, technology investment can mitigate CO_2 emissions from upstream city clusters. In conclusion, this study provides a scientific basis for developing CO_2 mitigation strategies for urban land within the YREB.

Keywords: urban expansion; spatial prediction; LSTM; geographical detector; driving factors

Citation: Wang, C.; Wang, J.; Ma, L.; Jia, M.; Chen, J.; Shao, Z.; Chen, N. Prediction Modeling and Driving Factor Analysis of Spatial Distribution of CO_2 Emissions from Urban Land in the Yangtze River Economic Belt, China. *Land* **2024**, *13*, 1433. https://doi.org/10.3390/land13091433

Academic Editor: Alexandru-Ionuţ Petrişor

Received: 7 August 2024
Revised: 29 August 2024
Accepted: 3 September 2024
Published: 4 September 2024

1. Introduction

Global warming presents a grave danger to human society and ecosystems, ranking among the most pressing environmental issues of our time [1,2]. Its primary driver is the emissions of greenhouse gases, such as CO_2 [3]. Despite covering only 2% of the planet's land area, urban areas are responsible for more than 60% of the emissions contributing to the greenhouse effect and utilize 78% of the world's energy supply [4]. Human activities and industrial processes in cities lead to energy consumption and consequently CO_2 emissions, indirectly impacting the urban climate and ecological environment [5–8]. China's

rapid urbanization and socioeconomic development in recent decades have significantly influenced terrestrial ecosystems and increased CO_2 emissions [9–12]. Urban land, as a critical area for human activities, has complex CO_2 emissions originating from various sources [13]. Understanding the spatial distribution of urban CO_2 emissions is vital for accurately estimating and predicting the growth trends and driving factors of CO_2 emissions under current socioeconomic development conditions, in order to formulate effective carbon reduction strategies [14,15].

Recently, there has been considerable research on the spatialization of urban CO_2 emissions [16–18]. These studies can be categorized into two primary methods: bottom-up and top-down [19]. Bottom-up methods face challenges, such as data scarcity, acquisition difficulties, and a lack of timeliness and universality, making them less applicable. In contrast, top-down methods benefit from readily available data and broader applicability [20,21]. Top-down methods can be further classified into two types. The first involves allocating CO_2 emission statistical values to grid cells using nighttime lights and other data sources. For example, some studies have proposed a grid allocation approach based on land-use types, which has been applied in specific cities [18,22]. Furthermore, Gao et al. [21] combined nighttime lights with electricity consumption to create an Energy and Emissions Comprehensive Index (EECI) for fine-scale CO_2 emission spatialization (130 m). Although effective in estimating CO_2 emission distributions, these methods have lacked a quantitative model assessment, limiting their predictive capabilities. The other type has established regression models between total CO_2 emissions at regional levels and statistical socioeconomic data, such as nighttime lights, to estimate the CO_2 emission distribution. For instance, Guo et al. [23] developed spatio-temporal regression models based on enhanced population-light index (RPNTL) data for urban, industrial, and rural areas, achieving a spatial CO_2 emission estimation. Additionally, indices, such as the Improved Vegetation Adjusted Nighttime Light Urban Index (VANUI) [24] and Improved CO_2 Emissions Index (ICEI) [25], have been proposed to estimate CO_2 emissions. Although the latter methods have enabled quantitative model evaluation and prediction extension, uncertainty in regression models may introduce deviations in estimation results [26]. The reason for this uncertainty is that while there is a high correlation between socioeconomic variables and CO_2 emissions, it is not possible to accurately estimate or predict grid-level CO_2 emissions based solely on socioeconomic variables.

Currently, there is limited research on spatially predicting future urban land CO_2 emissions. For instance, considering the variation in urban population density, an estimation of the prospective spatial arrangement of population density is made, and then, the total CO_2 emissions plan from the Intended Nationally Determined Contributions (INDC) is allocated to grid cells [27]. However, this method is too simplistic and cannot evaluate the precision of the predicted outcomes. Luo et al. [28] used ridge regression to correlate CO_2 emissions with land-use proportions, predicting emissions in Xi'an City. However, this method lacks temporal data validation and wide spatial coverage. Deep-learning LSTM models, as Huang et al. [29] demonstrated, address these limitations. Previous research indicates the potential of nighttime lights and population data for estimating urban CO_2 emissions, as these metrics closely reflect human activity intensity, which is closely tied to emissions [30–32]. Thus, using socioeconomic grid data, such as nighttime lights and the population, with LSTM models offers promise in predicting future urban CO_2 emission patterns.

Moreover, many studies that examine the effects of urban expansion on CO_2 emissions rely on historical data to analyze this relationship. For instance, the analysis of how urban expansion affects CO_2 emissions [33] and the trade-off between urban land expansion and ecological development concerning CO_2 emissions [34] demonstrate important relationships. However, there is limited research on the potential factors influencing future urban expansion and CO_2 emissions. Identifying these driving factors can enhance the understanding of CO_2 emissions from urban land expansion, laying the groundwork for future reductions in urban CO_2 emissions and sustainable development [35].

In this study, a method for predicting the spatial distribution of urban land CO_2 emissions was proposed based on CO_2 emission statistical data and urban socioeconomic grid data. An LSTM model with additional fully connected layers was applied in the method to predict the spatial distribution of CO_2 emissions from urban land. Urban land CO_2 emissions are correlated to socioeconomic grid data. Due to their high magnitude and extensive coverage, urban land CO_2 emissions represent a significant component of overall urban CO_2 emissions [36]. The urban land in this study refers to residential, commercial, and public spaces within a city, excluding industrial areas. Taking the YREB as the study area, this study predicted the spatial distribution of urban land CO_2 emissions for the year 2030 based on nighttime lights (NTL), population (POP), Gross Domestic Product (GDP), electricity consumption (EC), and land use data. Furthermore, the potential driving factors of the increase in CO_2 emissions from urban land expansion from 2020 to 2030 were analyzed based on the geographical detector. The aims of this study are as follows: (1) to develop a CO_2 emissions spatial distribution prediction model based on socioeconomic grid data; (2) to predict and analyze the spatio-temporal evolution of CO_2 emissions within the YREB; (3) to explore the potential factors driving future urban land expansion CO_2 emissions, providing a scientific basis for low-carbon and sustainable development of cities.

2. Materials and Methods

2.1. Research Framework

The study framework comprises three main sections: data collection and preprocessing, model training and prediction, and spatio-temporal analysis of results (Figure 1). In the data collection and preprocessing phase, socioeconomic grid data, land use data, and statistical yearbook data are preprocessed. For model construction and training, an integrated LSTM model was developed using time-series socioeconomic data and urban land CO_2 emissions statistics. This model aimed to predict the spatial distribution pattern of urban land CO_2 emissions for 2030, leveraging historical data. In the driving analysis, a geographical detector model was utilized to identify the driving factors, such as the end-of-year urban population and population density, affecting the increase in CO_2 emissions and the decrease in carbon sequestration from urban land expansion. Additionally, a spatial and temporal analysis for all the cities and only provincial capital cities was conducted to offer insights and recommendations for urban development.

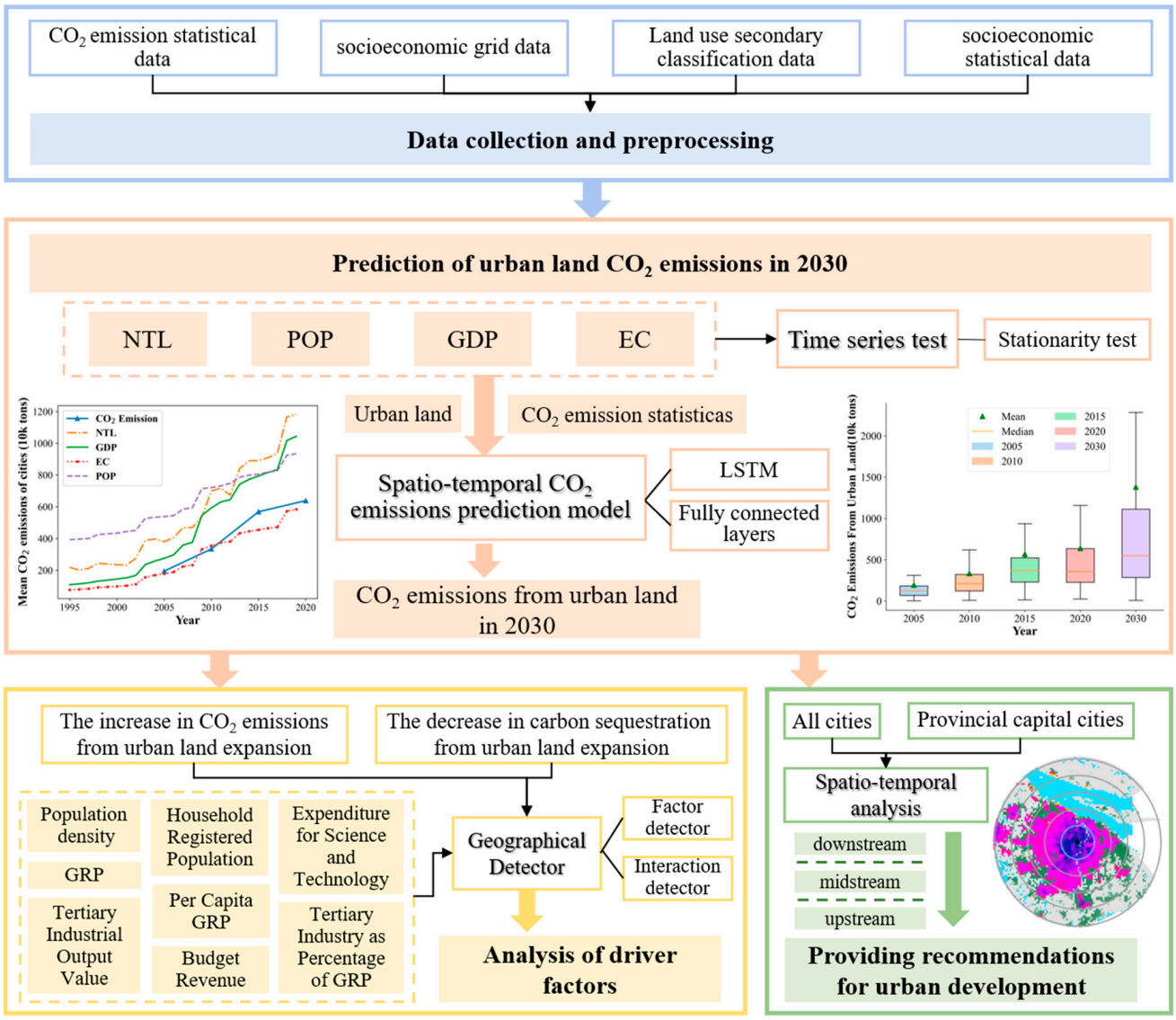

Figure 1. The workflow of the study.

2.2. The Study Area

The YREB stretches across China's eastern, central, and western areas, encompassing 11 provinces and municipalities, such as Shanghai, Wuhan, and Chengdu. It covers an area of about 2.0523 million square kilometers and is situated between latitude 21° 08′ N–35° 08′ N and longitude 97° 21′ E–122° 12′ E (Figure 2). With its population and GDP collectively representing over 40% of China's total, the YREB holds significant influence as an inland-river economic development zone on a global scale [37]. Known for its concentration of modern industries, such as steel, automobiles, and electronics, the belt boasts a high urban density, with urbanization levels around 50% and urban density 2.16 times higher than the national average, transforming it into one of the most economically prosperous areas beyond the coastal regions.

The YREB is divided into three regions based on the river basin topography and administrative boundaries: the downstream, midstream, and upstream areas [38]. The downstream cities feature a flat terrain, high population density, and advanced urbanization, contributing to about 25% of China's socioeconomic output, despite covering less than 4% of the land [39]. The midstream cities are characterized by a hilly and plain topography, with a large population and rapid urban development [40]. The upstream cities have a complex topography, including basins, mountains, and plateaus. Economic development and urbanization levels are relatively underdeveloped, and urban development is uneven [41].

The belt's rapid urbanization and expansion, along with the increasing population density and traditional energy consumption, have led to a notable surge in CO_2 emissions [42]. The rapid development of the YREB has come at the cost of excessive resource consumption and is currently facing issues of excessive CO_2 emissions, particularly in the downstream provinces and major cities [43,44]. The belt is now actively advancing a strategy of "taking concerted efforts to achieve ecological protection" and aims to become a leading area for ecological civilization in China [45]. Therefore, taking the YREB as a demonstration area to study urban land CO_2 emissions and their driving factors holds significant importances for carbon reduction in other cities in China and around the world.

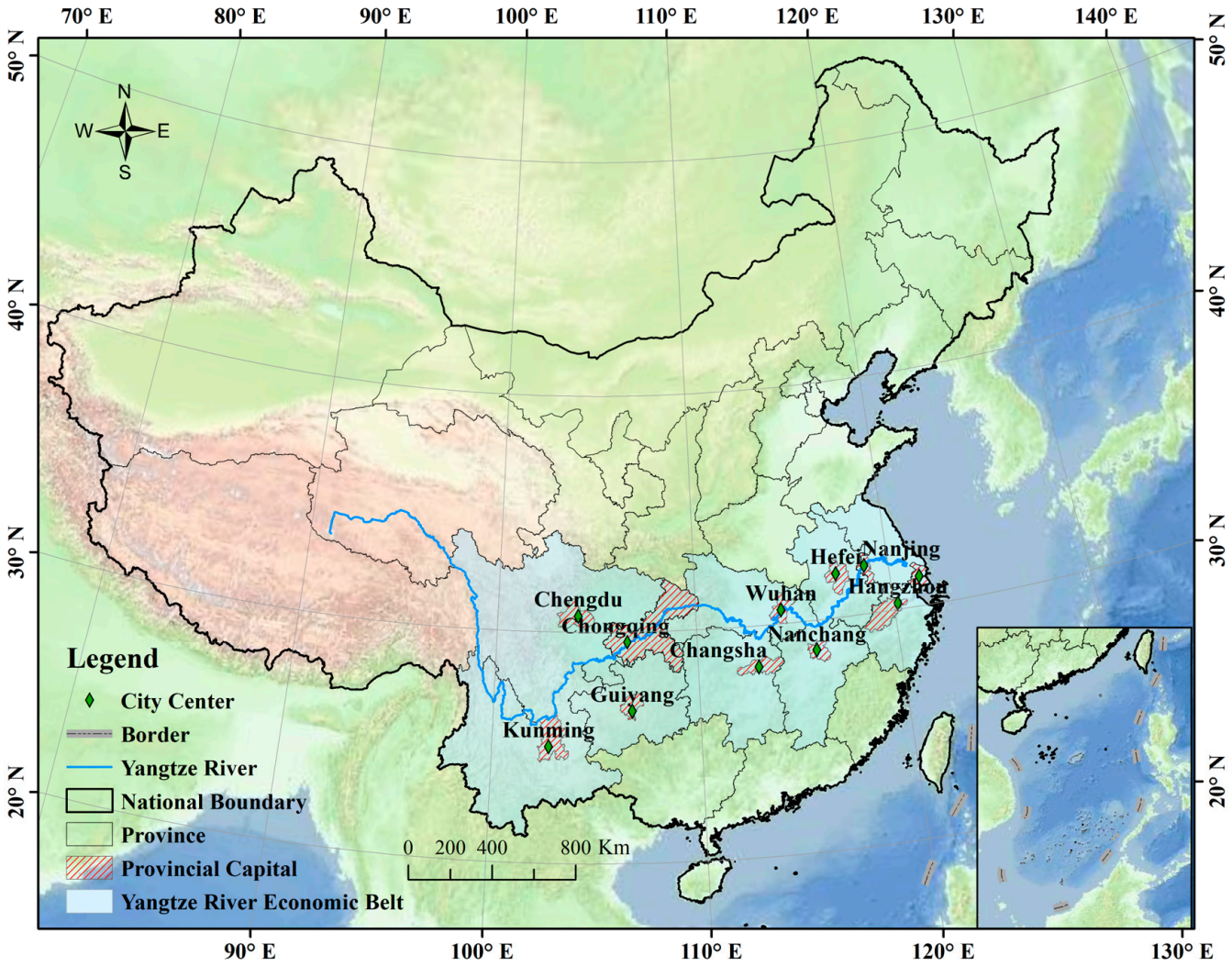

Figure 2. Study area.

2.3. Data Sources and Preparation

The CO_2 emission dataset, socioeconomic grid datasets, land use, and socioeconomic statistical datasets were employed in this study (Table 1). CO_2 emission data at the prefectural city scale spanning from 2005 to 2020 was obtained from the China City Greenhouse Gas Working Group (http://www.cityghg.com/, accessed on 12 October 2023). These data were used as the basis for CO_2 emission predictions related to urban land use. Socioeconomic grid data comprised nighttime light data from 1995 to 2019 sourced from the National Earth System Science Data Center (https://www.geodata.cn/main/, accessed on 3 November 2023), population grid data from 2000 to 2019 from WorldPOP (https://hub.worldpop.org/, accessed on 8 November 2023), and electricity consumption and GDP grid data from 1995 to 2019 from Chen and Gao [46]. These socioeconomic grid

datasets were projected to the Albers coordinate system with a 1 km spatial resolution. Land-use data with detailed classification criteria from 2000 to 2020 were obtained from the Institute of Geographic Sciences and Natural Resources Research, Chinese Academy of Sciences. Urban land simulation data for 2030 were provided by PANGAEA's Data Publisher for Earth & Environmental Science [47]. The socioeconomic statistical datasets comprise eight potential factors that may affect the increase in CO_2 emissions from urban land expansion, including the household registered population at year-end, population density, Gross Regional Product (GRP), per capita GRP, local general public budget revenue, expenditure for science and technology, tertiary industry as a percentage of the GRP, and tertiary industrial output value, all sourced from the 2019 Chinese City Statistical Yearbook (https://data.cnki.net/, accessed on 10 December 2023).

Table 1. Overview of datasets utilized for this study.

Type	Data	Year	Source
CO_2 emission data	CO_2 emission statistics	2005, 2010, 2015, 2020	China City Greenhouse Gas Working Group
Socioeconomic grid data	Nighttime light	1995–2019	National Earth System Science Data Center
	Population	2000–2019	WorldPOP
	GDP	1995–2019	Chen and Gao [46]
	Electricity consumption	1995–2019	
Land use data	Secondary land use classification (Urban land)	2000, 2005, 2010, 2015, 2020	Institute of Geographic Sciences and Natural Resources Research, Chinese Academy of Sciences
	Future urban land	2030	PANGAEA
Socioeconomic data	Household registered population at year-end (HRP) Population density (PD) Gross Regional Product (GRP) Per capita GRP (PGRP) Local general public budget revenue (BR) Expenditure for science and technology (EST) Tertiary industry as percentage of GRP (TIGRP) Tertiary industrial output value (TI)	2019	China City Statistical Yearbook

CO_2 emissions can be divided by land-use type into three categories: urban land, industrial land, and rural land [32]. This study focuses on the spatial prediction of CO_2 emissions from urban land use. Urban land includes transportation land, residential land, commercial and service land, and construction land. CO_2 emissions corresponding to urban land use include emissions from the service industry, urban living, transportation (road, rail, water transport, aviation), and some indirect emissions. Only a few cities have indirect CO_2 emissions in the CO_2 emission statistics, which cannot be allocated to urban land or industrial land, and since their magnitude is small, half of the indirect CO_2 emissions are allocated to urban land.

2.4. Methodology

2.4.1. Stationarity Test

Stability tests are conducted on the time-series data of each variable to ensure stationarity, essential for predicting future CO_2 emissions. Before conducting tests, socioeconomic grid data are aggregated by the city. The urban land area is extracted using land-use data from 1995 to 2020 at five-year intervals. Missing years are replaced with the nearest available land-use data. This process yields annual urban land CO_2 emissions for 126 cities, which are then averaged to obtain a time series of the total value of socioeconomic grid data.

The Augmented Dickey–Fuller (ADF) test is employed to assess time-series stationarity, overcoming limitations of the Dickey–Fuller test in handling sequences with high-order lag terms and addressing autocorrelation in random disturbance terms.

$$Y_t = \alpha + \gamma t + (\rho - 1)Y_{t-1} + \sum_{i=1}^{k} \beta_i Y_{t-i} + \varepsilon_t \quad (1)$$

$$t_{\hat{\rho}} = \frac{\hat{\rho} - 1}{se(\hat{\rho})}, \quad t_{\hat{\alpha}} = \frac{\hat{\alpha} - 0}{se(\hat{\alpha})}, \quad t_{\hat{\gamma}} = \frac{\hat{\gamma} - 0}{se(\hat{\gamma})} \tag{2}$$

where $t_{\hat{\rho}}$, $t_{\hat{\alpha}}$, and $t_{\hat{\gamma}}$ follow the ADF distribution, which is used to test whether the original time series is a unit root process ($\rho = 1$). *se* represents the standard error, which is used to compute these test statistics.

2.4.2. The CO_2 Emission Spatio-Temporal Prediction Model

Socioeconomic grid data have been proven to have a substantial correlation with the spatial pattern of CO_2 emissions. Thus, they can be utilized for estimating and predicting the spatial distribution CO_2 emissions. To improve the precision of predicting the spatial distribution of urban land CO_2 emissions, this research proposes a spatial prediction model that integrates CO_2 emissions with nighttime light, population, electricity consumption, GDP, and land-use data (Figure 3).

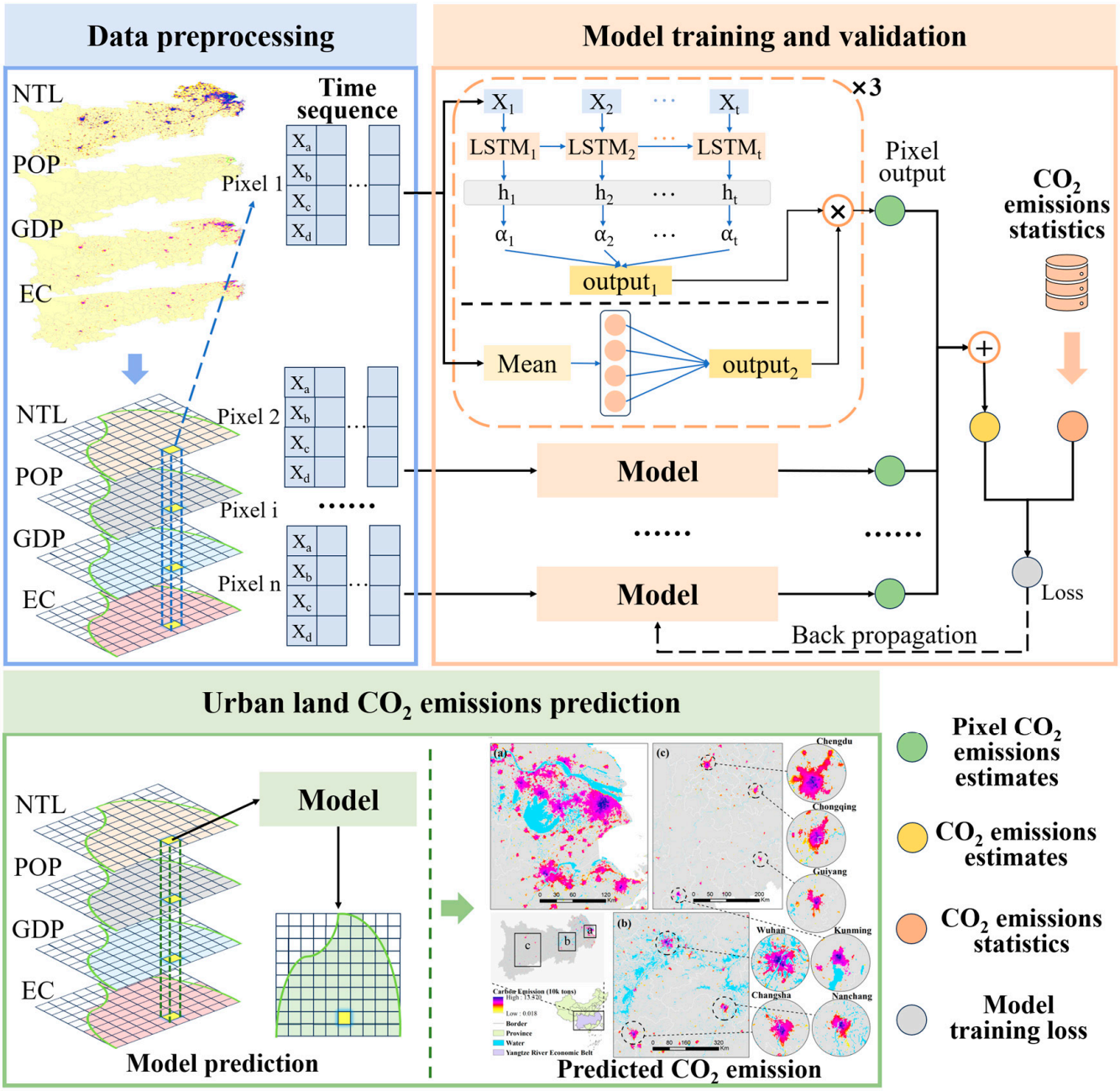

Figure 3. Spatio-temporal CO_2 emissions prediction model.

The LSTM model, a variant of the RNN model, addresses the problem of long-term dependency in RNNs by using "gate" units to control the updating or discarding of input data [48]. In this study, LSTM serves as the base model for predicting CO_2 emissions in 2030 based on socioeconomic grid data. However, since the model training is many-to-one, where pixel CO_2 emissions correspond to total city CO_2 emissions, it cannot ensure the spatial correlation between the output CO_2 emissions and the socioeconomic grid data. To address this, a fully connected layer module is integrated into the model. This module averages the input socioeconomic grid data, calculates weight coefficients, applies them multiplicatively to the model's output, and keeps its parameters fixed during mid-term training. Furthermore, to enhance prediction accuracy and stability, an ensemble model that averages predictions from multiple models is employed. The model description is as follows:

$$\hat{CE}_i = f_3\left[f_1(x_{1i}, x_{2i}, x_{3i}, x_{4i}) f_2\left(\frac{\sum_{j=1}^{n} x_{1ij}}{n}, \frac{\sum_{j=1}^{n} x_{2ij}}{n}, \frac{\sum_{j=1}^{n} x_{3ij}}{n}, \frac{\sum_{j=1}^{n} x_{4ij}}{n}\right)\right] \quad (3)$$

$$CE_{city} = \sum_{i=1}^{N} \hat{CE}_i + \varepsilon \quad (4)$$

where x_{1ij} represents the time-series data of the first input variable based on the ith pixel for the jth year, where n represents the length of the time series, N represents the total number of pixels for urban land use in the city, $\hat{CE}_i$ represents the estimated CO_2 emission of the output pixel, and CE_{city} represents the statistical value of city CO_2 emissions. f_1 represents the LSTM model, f_2 represents the fully connected layer module, and f_3 represents the ensemble model.

$$MSELoss = \frac{\sum_{i=1}^{m} (y_i - \hat{y}_i)^2}{m} \quad (5)$$

During model training, we utilize the $MSELoss$ loss function, where y_i represents the actual CO_2 emission value and $\hat{y}_i$ represents the predicted CO_2 emission. The socioeconomic grid data from 1995 to 2004 and 2000 to 2009 are associated with CO_2 emissions in 2015 and 2020, respectively, serving as the training dataset. Data from 2010 to 2019 correspond to CO_2 emissions in 2030 and are utilized for prediction purposes.

2.4.3. Geographical Detector

The geographical detector, a statistical model based on spatial variance analysis, has garnered widespread adoption within the realm of spatial analysis [49,50]. This study uses the factor detector and interaction detector models of the geographical detector to explore the potential influence of factors on the spatial distribution of the increase in CO_2 emissions and the decrease in carbon sequestration due to urban land expansion from 2020 to 2030, as well as the interaction between multiple factors. The geographical detector is implemented using the R language GD library (https://CRAN.R-project.org/package=geodetector, accessed on 5 January 2024).

The factor detector is used to identify spatial disparities among variables and to assess the extent to which factors contribute to these spatial variations [51].

$$q = 1 - \frac{\sum_{h=1}^{L} N_h \sigma_h^2}{N\sigma^2} = 1 - \frac{SSW}{SST} \quad (6)$$

In the formula, q represents the impact level of factors on the spatial heterogeneity of the target variable, ranging from 0 to 1, with a higher value indicating a greater explanatory power of factors on the spatial heterogeneity of the target variable; $h = 1, 2, \ldots, L$ represents the partition of variables or factors, N_h and N represent the count of units in the partition and the overall count of units in the whole area, respectively, σ_h^2 and σ^2 represent the variance within the partition and the total variance of the whole area, respectively, SSW and SST represent the sum of squares within the partition and the total sum of squares of the whole area, respectively.

The interaction detector is used to identify interactions among various factors and to evaluate whether the combined effect of two factors on a variable enhances or diminishes

the explanatory capacity of the variable. The q value of the factors' influence on the variable (q(x1) and q(x2)) is initially determined, followed by the calculation of the q value for the layer resulting from the interaction between the two factors (q(x1∩x2)). The relationship among q(x1), q(x2), and q(x1∩x2) is to be determined, and the type of interaction is to be determined as well [52].

3. Results

3.1. The Prediction Results

The changes in time-series data used in this study were analyzed. Figure 4 depicts the changes in socioeconomic grid data and CO_2 emissions after the data were normalized to the same range. The average CO_2 emissions from urban land in the YREB saw a significant rise from 2005 to 2020, especially during 2005–2015. The rate of increase in CO_2 emissions has risen by an average of 51.41% for each five-year interval. From 1995 to 2019, the mean values of urban land-use socioeconomic grid data show a clear increasing trend, indicating growth in the urban land expansion, population, GDP, and electricity consumption. The average growth rates are 7.93%, 3.80%, 10.38%, and 9.28%, respectively. This growth trend correlates with CO_2 emissions, supporting the use of socioeconomic grid data to predict urban land CO_2 emissions.

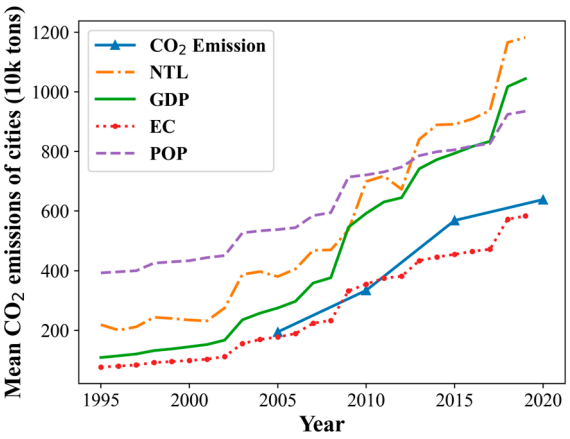

Figure 4. Change in data in urban land from 1995 to 2020.

For the stationarity test of socioeconomic grid data and CO_2 emissions over time (Table 2), all four variables failed the unit root ADF test, confirming that the original variables were non-stationary. However, after first-order differencing, the data became stationary, enabling the prediction of CO_2 emissions utilizing these time-series data.

Table 2. Time-series stationarity test.

Variables	ADF Test	
	Intercept and trend	Intercept and trend
	Level	1st difference
Nighttime Light (NTL)	0.999	5.88×10^{-5}
Population (POP)	0.985	6.40×10^{-7}
Gross Domestic Product (GDP)	0.997	2.95×10^{-5}
Electricity Consumption (EC)	0.995	1.00×10^{-5}
CO_2 Emissions (CE)	0.858	- *

*: Due to the limited four-year span of CO_2 emissions data, the series after differencing is too short for testing.

Over the last 25 years, urban land in the YREB has consistently expanded, mainly in the Yangtze River Delta region, particularly Shanghai and Suzhou. Meanwhile, national initiatives, such as the "Revitalization of Central China" and the "Western Development"

have further accelerated urban land expansion in the middle and upper regions of the Yangtze River [53].

Figure 5 depicts the predicted spatial distribution of urban land CO_2 emissions in cities across the YREB in 2030. It reveals that CO_2 emissions are notably higher in the central city areas and gradually diminish towards rural regions. Urban land CO_2 emissions range from 0.18 to 133.70 k tons/grid, with an average of 42.18 k tons and a standard deviation of 17.89 k tons. Grids with CO_2 emissions ranging from 30 to 70 k tons/grid are widely distributed around urban core areas, accounting for over 70%. Grids with CO_2 emissions exceeding 70 k tons/grid are concentrated in core areas, particularly in economically developed cities, accounting for approximately 3%. Grids with CO_2 emissions below 30 k tons/grid are scattered in suburban and town areas. From 2020 to 2030, expansion land CO_2 emissions range from 0.18 to 114.28 k tons/grid, with a mean of 34.70 k tons and a standard deviation of 17.30 k tons. CO_2 emissions from urban land expansion account for 33.14% of the total urban land CO_2 emissions. This phenomenon is more severe in the Yangtze River Delta region, where it accounts for 41.12%.

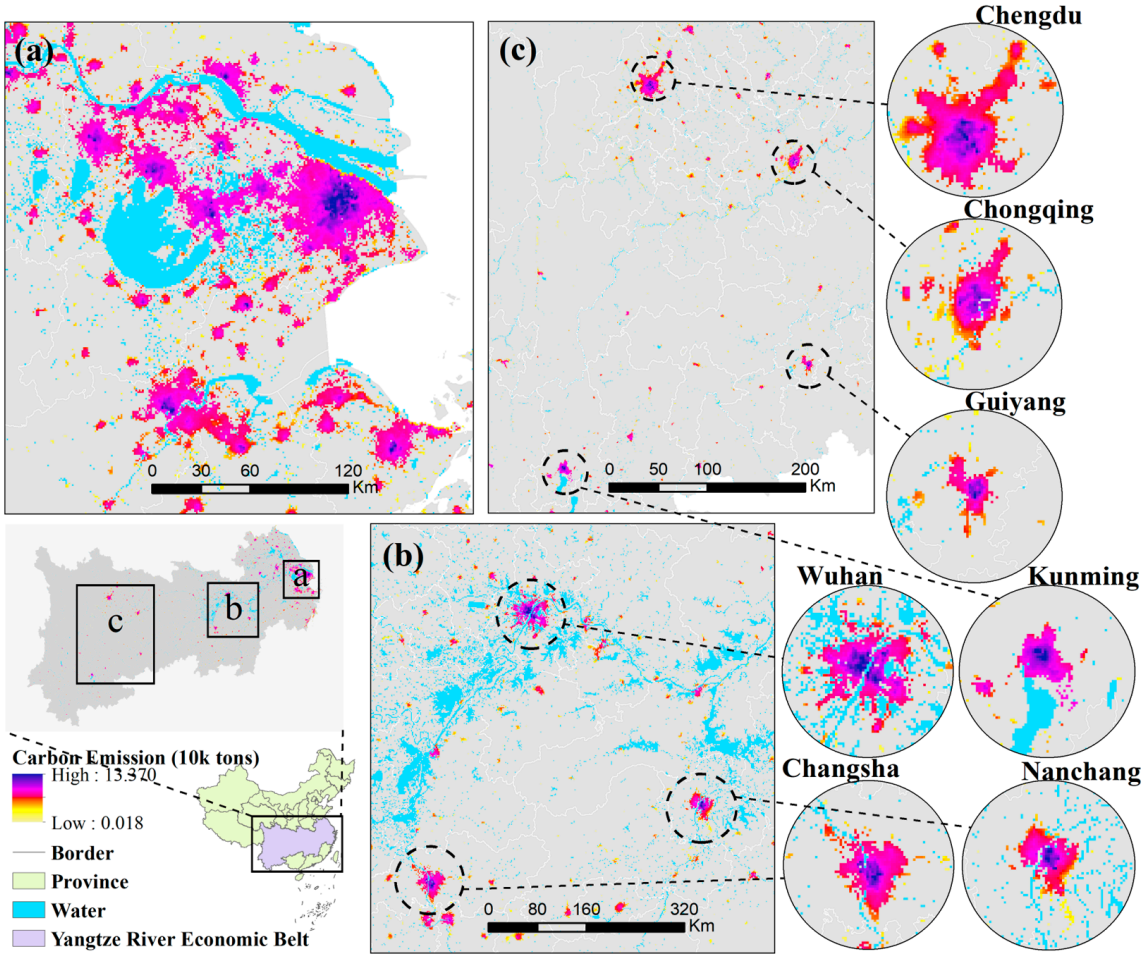

Figure 5. Spatial distribution of urban land CO_2 emissions in the YREB in 2030. (**a**), (**b**), and (**c**) are the lower, middle, and upper reaches, respectively.

Cities in the lower reaches of the Yangtze River display widespread high CO_2 emissions due to their large urban land area and concentrated emission sources, resulting in higher overall emissions compared to other areas. The Yangtze River Delta has experienced swift development and high population density recently. This population surge is anticipated to boost the consumption of fossil fuels, consequently generating substantial CO_2 emissions [25]. Conversely, cities in the middle and upper reaches exhibit high CO_2

emissions mainly in their central areas. Due to their smaller and less concentrated urban land, these cities have lower total CO_2 emissions.

3.2. Spatio-Temporal Variation Characteristics of CO_2 Emissions

From 2005 to 2030, urban land CO_2 emissions in cities across the YREB have generally risen (Figure 6). In 2030, the average CO_2 emissions are projected to be 13805.42 k tons, with a median of 5483.54 k tons (Figure 6a). The ten-year average growth rate of CO_2 emissions is 103.73%. Specifically, the average growth from 2020 to 2030 is 7420.90 k tons, with a growth rate of 116.23%. This indicates that urban land CO_2 emissions in the YREB will continue to increase from 2020 to 2030.

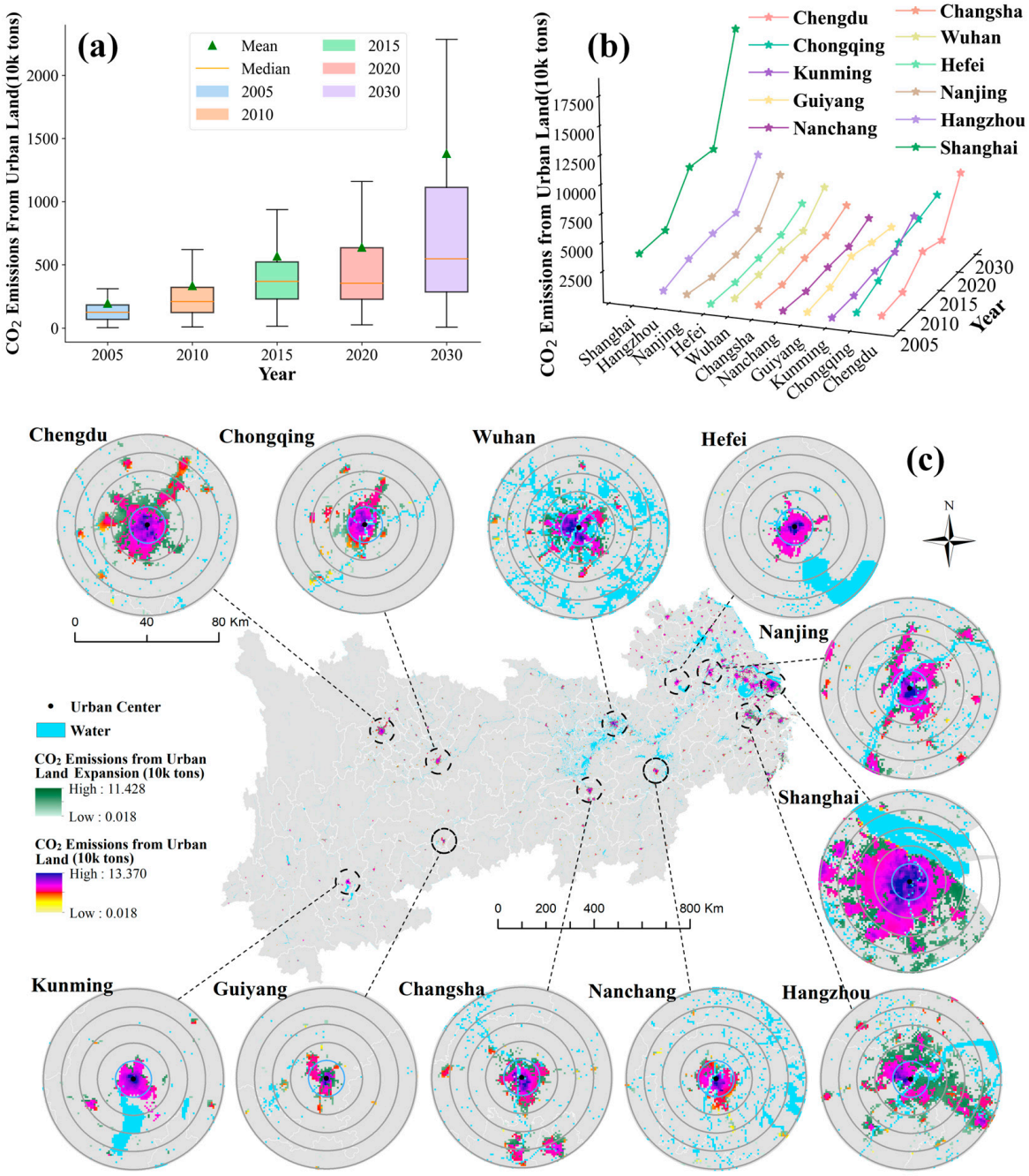

Figure 6. Results of spatio-temporal changes: change in CO_2 emissions in all cities (**a**), change in CO_2 emissions in provincial capital cities (**b**), and spatial distribution of CO_2 emissions from urban land and urban land expansion in provincial capital cities (**c**).

Analyzing the CO_2 emission changing trends of provincial capitals within the YREB (Figure 6b,c), significant increases were observed in Nanjing, Hangzhou, and Shanghai, with the exception of Hefei. The urban regions on the eastern seaboard of the Yangtze River Delta, as well as the more developed central areas, are experiencing a rapid increase in CO_2 emissions [54]. It is projected that Shanghai, Hangzhou, and Nanjing will expand outward significantly from 2020 to 2030, resulting in a substantial rise in CO_2 emissions by 2030. These cities are expected to experience a CO_2 emissions growth rate of over 200% from 2020 to 2030. Changsha and Nanchang show consistent increase in emissions with a slight uptick expected by 2030, with a CO_2 emission growth rate of about 100%. In the cities along the middle reaches, urban expansion exerts a more pronounced impact on driving CO_2 emissions than economic growth [10]. Chengdu and Chongqing will experience significant urban expansion leading to increased CO_2 emissions, especially in Chengdu, by 2030. Kunming's CO_2 emissions are rising due to positive lifestyle and economic trends despite minimal urban expansion. Emissions in Guiyang increased slightly from 2005 to 2015 but are expected to decrease by 9.86% by 2030 due to declining population density and active promotion of low-carbon living.

From 2020 to 2030, urban land CO_2 emissions in the upper and middle reaches show a gradual increase, although some cities observe a slight decline in emissions. The increasing demand for urban residents' lifestyles, including food, transportation, and shopping, contributes to the rise in CO_2 emissions from urban land. Simultaneously, the vigorous promotion of low-carbon living partially suppresses the unlimited growth of CO_2 emissions. Thus, the observed gradual rise in urban land CO_2 emissions aligns with the expected outcomes of the study. In contrast, the significant increase in CO_2 emissions in the lower reaches from 2020 to 2030 is partly due to the robust economic development, rapid population growth, and intense urban expansion in these cities.

3.3. Driving Factors of the Increase in CO_2 Emissions and the Decrease in Carbon Sequestration

This study explores how different socioeconomic factors impact the increase in CO_2 emissions and the decrease in carbon sequestration when cities expand their land areas (Figure 7). It also found that several socioeconomic factors positively impact the increase in CO_2 emissions from urban land expansion in the YREB (Figure 7a). Among these factors, GRP, BR, TI, and EST are identified as primary influencers, with q-values exceeding 0.7, while PD had the smallest impact, with a q-value as low as 0.1. In interaction detection, TI and PD, BR and PD, and PGRP and PD all exhibit nonlinear enhancement effects, with their combined effects on the dependent variable reaching 0.92, 0.90, and 0.8,7 respectively (Figure 7b). This indicates that while PD does not directly affect the increase in CO_2 emissions from future urban land expansion, it serves as a foundational factor. Overall, the future increase in CO_2 emissions resulting from urban land expansion will mainly be influenced by the current population density, the state of service industry development, technological investment, and residents' living standards, with GRP being the dominant driving factor.

Furthermore, the analysis identified potential factors contributing to the decrease in carbon sequestration from urban land expansion. The direct impact of these socioeconomic variables is relatively small, with BR being the primary direct influencing factor, with a q-value of less than 0.5 (Figure 7c). Interaction detection shows that the linear enhancement effect of TIGRP and PGRP on the dependent variable is the greatest, reaching 0.62, whereas their individual effects are only 0.4 (Figure 7d). This indicates that the urban economic structure and residents' living standards jointly influence the decrease in carbon sequestration from urban land expansion. Additionally, similar to the driving analysis of the increase in CO_2 emissions, PD's nonlinear enhancement effects with both TI and BR also contribute significantly to explaining the variance in the dependent variable, each reaching 0.6. Therefore, when urban PD reaches a certain level and economic development is robust, further expansion of urban land becomes necessary, leading to a reduction in carbon sequestration.

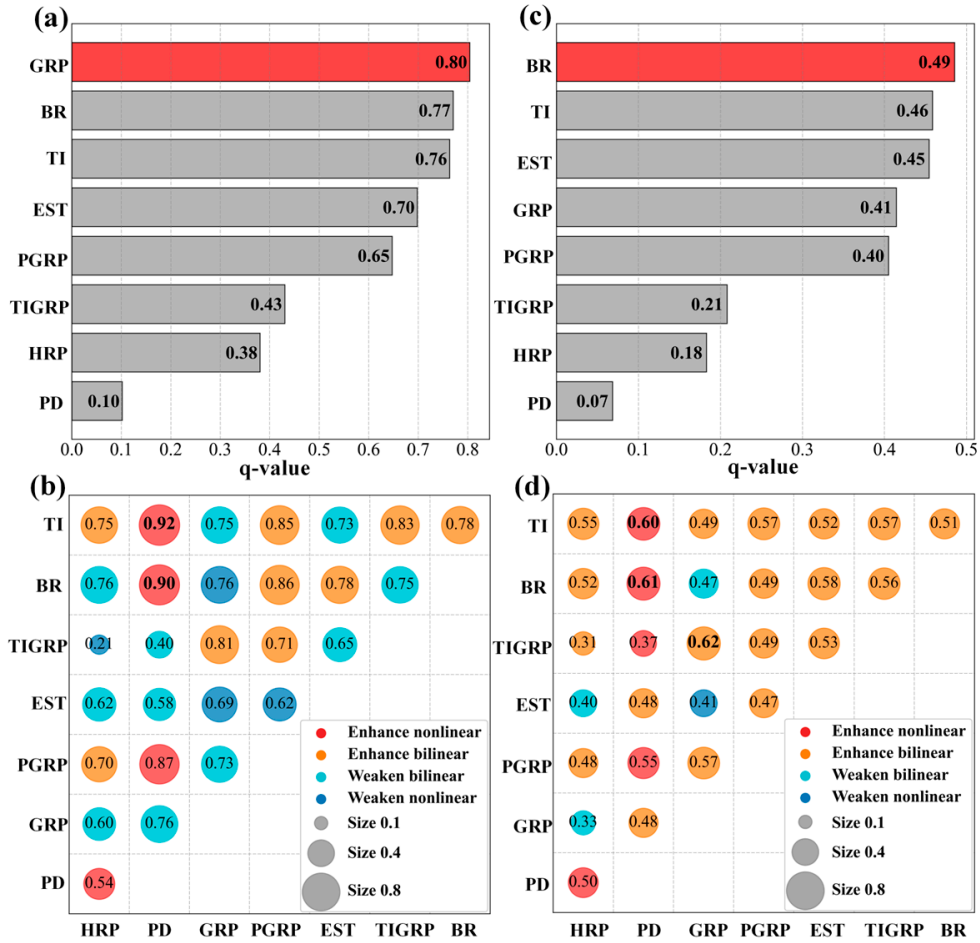

Figure 7. Results of the driving factors analysis: factor detector (**a**,**c**) and interaction detector (**b**,**d**); (**a**,**b**) represent the increase in CO_2 emissions from urban land expansion, and (**c**,**d**) represent the decrease in carbon sequestration from urban land expansion from 2020 to 2030.

4. Discussion

4.1. Model Evaluation and Result Analysis

Due to uncertainties, some cities experience overestimation or underestimation when predicting CO_2 emissions using socioeconomic grid data [55]. Figure 8 illustrates the model's fitting performance for total urban land CO_2 emissions in 2015 and 2020, evaluating the model's fitting effectiveness in different regions and cities based on fitting deviations. The study shows that the method used is generally accurate, with an overall R-squared of 0.73 for urban areas in cities along the YREB in 2015 and 2020. The highest accuracy is in the midstream city cluster, with an R-squared of 0.84, while the upstream and downstream city clusters have R-squared values of 0.69 and 0.75, respectively, indicating the model's reliability (Figure 8c–f).

Most overestimated cities are in the lower reaches, covering most of Jiangsu Province and some cities in Zhejiang and Anhui provinces (Figure 8a,b). In the urban agglomeration of the lower reaches, the average values of absolute and relative deviations in CO_2 emissions are 209.01 (10 k tons) and 0.23, respectively. Notably, Suzhou, Nanjing, and Ningbo show high socioeconomic grid data, such as nighttime light, due to their large urban areas, dense populations, and strong economies [56]. This overestimation is primarily due to the dominance of small cities in the YREB. Additionally, some larger cities, despite their efforts in emission reduction, are also overestimated due to their socioeconomic data. For instance, Shanghai is underestimated in 2015 but overestimated in 2020. In the early 21st century, Shanghai experienced rapid urbanization, with significant population and economic growth. With the implementation of national measures for reducing CO_2

emissions and the development of green and low-carbon technologies, cities are expected to gradually reduce the growth rate of CO_2 emissions [57].

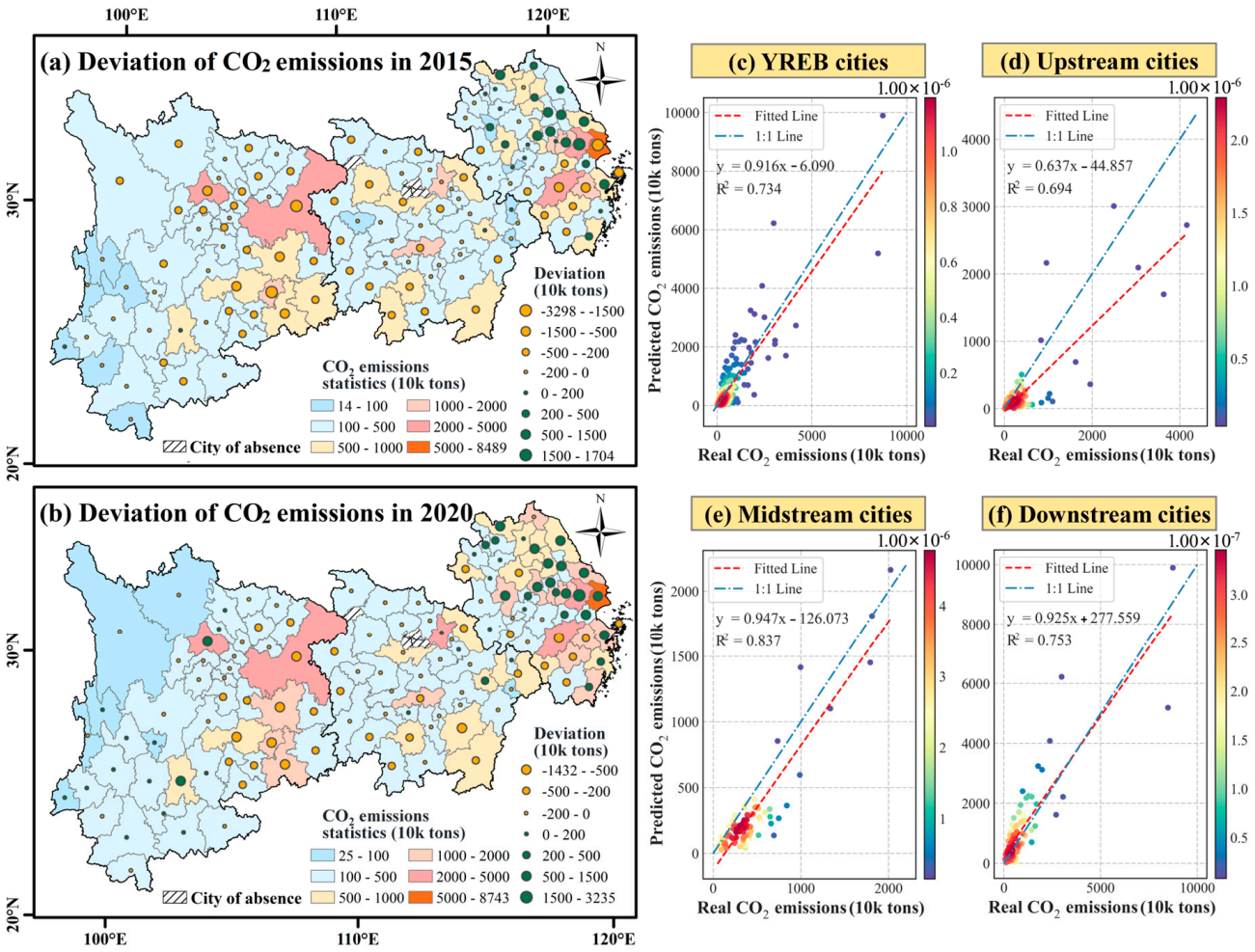

Figure 8. The performance of model fitting. (**a**) and (**b**) represent the spatial distribution of model fitting deviations for 2015 and 2020. (**c**), (**d**), (**e**), and (**f**) represent the deviations of all cities, upstream cities, midstream cities, and downstream cities, respectively.

Underestimated cities are mainly found in the upper and middle reaches and some cities in Zhejiang Province (Figure 8a,b). In the urban agglomerations of the middle and upper reaches, the average values of the absolute and relative deviations in CO_2 emissions are −185.35 (10 k tons) and 0.39, respectively. These underestimated cities are characterized by small urban land areas, low urban populations, and relatively low Nighttime Light Digital Number (DN) values, resulting in underestimated CO_2 emissions. Small cities constitute the majority of underestimated cities, leading to a relatively large relative underestimation deviation due to their small total CO_2 emissions. Notably, economically developed cities, such as Chongqing, Guiyang, and Hangzhou experience underestimated CO_2 emissions due to statistical errors in urban land area and CO_2 emissions. However, despite these deviations, the total CO_2 emissions of these cities are substantial, and the relative deviations are small, so the results remain credible.

The model fits best in the middle reaches of the city, most of the upper reaches, and the southern part of the downstream city (Figure 8a,b). However, the fitting effect is relatively poor in the northern part of the downstream city. The cities with poor fitting effects are mainly located in Jiangsu Province, where the economic development is good, the total CO_2 emissions are high, and they are generally overestimated. Due to the large total volume, the relative deviation of the estimated value is still credible. The cities with good model

estimation effects have an undulating terrain and moderate economic development. In these cities, the R-squared of the model test results can reach 0.87.

Overall, the absolute values of the average fitting deviations of the model across various regions do not exceed 210 (10 k tons), which is significantly less than the total CO_2 emissions of most cities. The R-squared of the model fitting in all simulated cities reaches 0.73. The estimated deviation in the middle reaches urban agglomeration is the smallest, with an R-squared value of 0.83. These results indicate that the model estimation accuracy meets the requirements. Therefore, the model can be used for predicting urban land CO_2 emissions in cities within the YREB. Additionally, the model performs well in areas with an undulating terrain and moderate economic development (most areas of YREB). Therefore, based on the applicability of this model, it can be expanded to more cities in the future.

The CO_2 emissions of the YREB from 2005 to 2030 are showing an upward trend (Figure 6a). The slight increase from 2015 to 2020 can be attributed to the impact of COVID-19, which reduced emissions due to decreased production and activities. The model predicts a significant increase in CO_2 emissions from urban land in the Yangtze River Delta region from 2020 to 2030 (Figure 6b,c), mainly due to the substantial expansion of urban land. These cities attract a large influx of population, leading to a continuous rise in population density, an increase in consumer spending power, the continuous expansion of urban land, and a reduction in terrestrial carbon sequestration [58,59]. According to the current development trend, the total CO_2 emissions from urban land in these cities will continue to rise, which is consistent with the results of related studies [60]. Compared to the Yangtze River Delta region, the urban land CO_2 emissions in the central reaches of the Yangtze River, such as Wuhan, Changsha, and Nanchang, are increasing steadily but at a slower pace. The increase in CO_2 emissions in these cities is mainly influenced by the expansion of urban land, hence the need to control urban land expansion to curb CO_2 emissions [1]. In the upper reaches of the Yangtze River, the CO_2 emissions from urban land in most cities no longer rise. However, in a few cities, such as Chengdu and Chongqing, the CO_2 emissions from urban land are still steadily increasing. This is due to the obvious urban expansion in these cities, and their CO_2 emissions from the service industry, urban living, and transportation are expected to rise with economic development.

4.2. Analysis of the Differences in Driving Factors of Urban Agglomerations in Different River Basins

Using geographical detectors, this study analyzed the drivers of CO_2 emission increases from urban land expansion in the Yangtze River's downstream, midstream, and upstream city clusters (Figure 9). The downstream cluster (Shanghai, Jiangsu, Anhui, Zhejiang) has a dense population and robust economy, with significant urban growth. The results indicate that the q-value of GRP reaches 0.85, while the q-value of PD is only 0.06. However, PD shows a nonlinear enhancement interaction with TI and BR, both at 0.97. This indicates that the increase in CO_2 emissions from downstream urban land expansion clusters is primarily driven by the population density and jointly influenced by economic and industrial development (Figure 9a,b). Population density is not a direct driver of increased CO_2 emissions from land expansion. This is attributed to the flat terrain and robust economic development in the Yangtze River Delta, where the population density is generally high across the cities. However, when cities have a well-developed economy and service industry, coupled with high population density, it directly leads to an increase in CO_2 emissions from land expansion, as exemplified by cities, such as Shanghai, Suzhou, and Hangzhou. Therefore, in the future, these cities will need to control urban land CO_2 emissions by restricting the increase in both population density and urban land area [61]. Additionally, it is essential to actively promote a green lifestyle, leveraging the advantages of technological development and population to collectively reduce CO_2 emissions [62]. The midstream cluster (parts of Hubei, Hunan, and Jiangxi), led by cities, such as Wuhan, Changsha, and Nanchang, has fewer people and less economic activity than the downstream area. The factor detection results indicate that the q-values of TI, GRP,

PGRP, and EST all exceed 0.85. Combined with the interaction detection, it shows that there is a linear-enhanced interaction among them, but it is not significant (Figure 9c,d). Interaction detection revealed that fiscal economic factors, rather than the population, are the primary drivers of CO_2 emissions from expanding land. The household registered population at year-end and population density do not exert a significant influence on the CO_2 emissions from urban land expansion. This is due to the stable development of the midstream urban agglomerations, where changes in the urban population are relatively minor compared to the downstream urban clusters, leading to a more stable pattern of urban expansion [63]. The factors that directly impact CO_2 emissions from land expansion are the city's service industry, per capita economic status, and fiscal revenue. In some cities within the midstream urban agglomeration, CO_2 emissions are trending towards stabilization or even decline. A few economically advanced cities need to pay attention to the expansion of urban land, especially in areas with vegetation coverage. The upstream cluster includes the Chengdu–Chongqing urban agglomeration, the Central Guizhou urban agglomeration, and the Central Yunnan urban agglomeration, characterized by a relatively underdeveloped economy and uneven urban development [64]. The factor analysis results suggest that the q-values for GRP, TIGRP, BR, and HRP all exceed 0.92, while EST is the lowest at 0.29 (Figure 9e,f). This indicates that economic development in upstream cities strongly drives urban expansion and CO_2 emissions. This is due to the complex terrain of the upstream urban agglomerations and the uneven urban development. Most cities have a smaller population, extensive areas of vegetation cover, and CO_2 emissions are tending to stabilize, with some cities experiencing a decrease in CO_2 emissions [65]. However, a few economically developed cities, such as Chengdu and Chongqing, still exhibit a trend in urban expansion, with increasing CO_2 emissions. Interaction detection analysis shows that these variables exhibit mutual attenuation, which is attributed to the uneven development of upstream city clusters. Notably, investment in science and technology can help mitigate urban land CO_2 emissions.

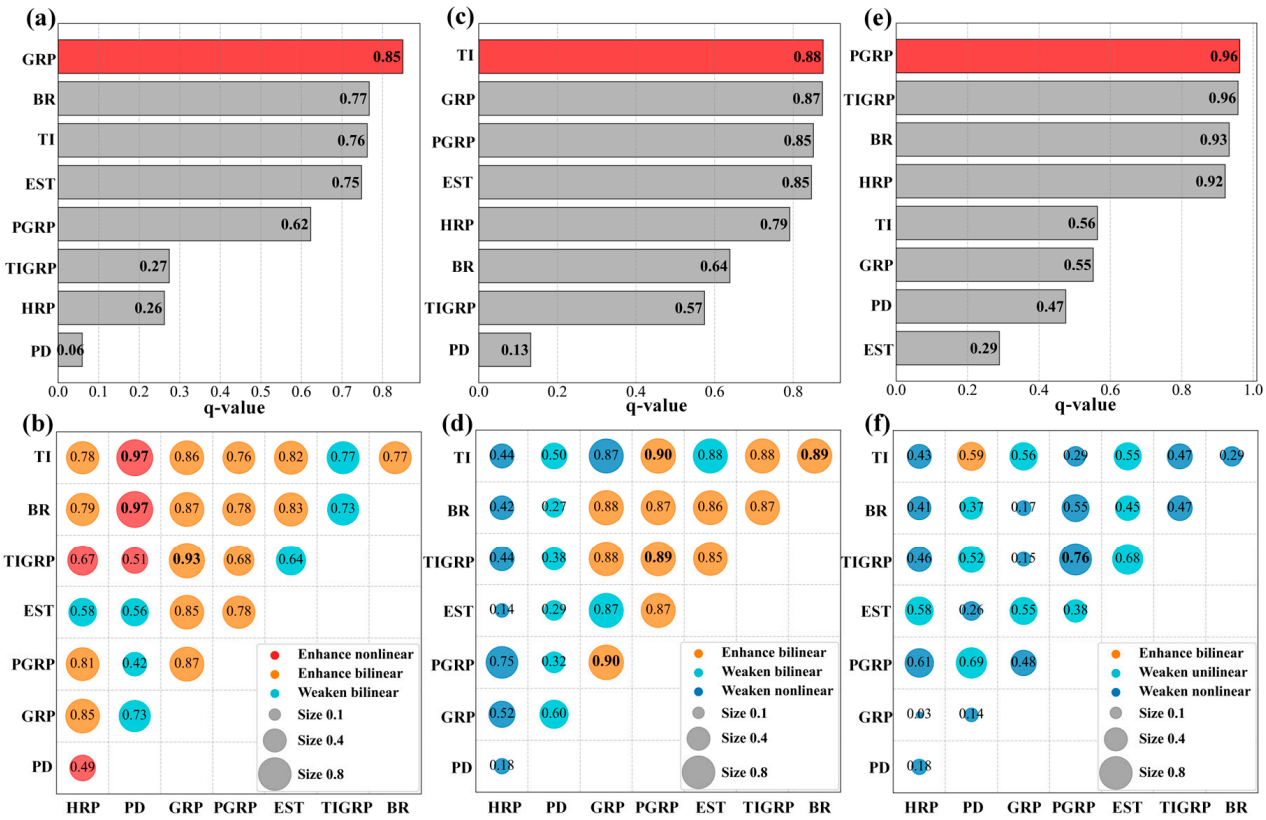

Figure 9. Results of the driving factors analysis: factor detector (**a**,**c**,**e**) and interaction detector (**b**,**d**,**f**). (**a**,**b**) represent downstream cities, (**c**,**d**) represent midstream cities, and (**e**,**f**) represent upstream cities.

In the downstream city cluster, particularly in cities such as Shanghai and Hangzhou, large-scale urban expansion is expected to result in higher CO_2 emissions in the future. To mitigate this, efforts to restrain urban land expansion should be accompanied by the development of multifaceted emission reduction strategies, including green building, energy conservation for urban residents, and the promotion of low-carbon transportation. Cities in the upper and midstream city clusters of the Yangtze River, with better fiscal and economic development, need to pay attention to urban land expansion. This expansion directly leads to increased CO_2 emissions, necessitating coordination between urban expansion and vegetation coverage. Increasing vegetation coverage alongside urban expansion not only reduces CO_2 emissions but also enhances the living environment [66]. Additionally, increasing investment in science and technology, as well as developing and promoting low-carbon products, can alleviate the pressure of CO_2 emission reductions from urban land to a certain extent.

4.3. Limitations and Implications

This study proposes a CO_2 emission spatial prediction model that uses various socioeconomic grid data and land-use data to predict the spatial distribution pattern of CO_2 emissions from urban land within the YREB in 2030. Compared to Wei et al. [32], this study utilizes multiple sources of socioeconomic grid data, enhancing the spatial capability of CO_2 emission prediction and extending its scope. Tao et al. [27] allocated total CO_2 emissions to a population grid for 2030 based on population change rates to determine the geographical spread of CO_2 emissions. In contrast, this study effectively utilizes the temporal features of data using the LSTM model and can assess the precision of the prediction model. Additionally, compared to Luo et al. [28], the model introduced in this research has wider applicability and can be employed to predict the spatial distribution pattern of CO_2 emissions for all cities within the YREB. Overall, this study provides a possibility for predicting the spatial distribution of urban land CO_2 emissions based on a deep learning model, and the predictive results within the YREB are credible.

There are also some limitations to our study. The model's application is limited to urban land due to weak correlations between socioeconomic data and CO_2 emissions from industrial and rural areas. It uses historical data to estimate emissions, but with national carbon policies and technology development, urban emissions are expected to decline and carbon intensity to fall. This study only predicts the future urban land CO_2 emissions based on the current societal scenario, without considering the impact of future development differences among various types of cities on CO_2 emissions. Additionally, city morphology and function also influence CO_2 emissions [23]. This study establishes a unified model for all cities, leading to certain biases in CO_2 emission predictions. There are certain limitations to this study that utilizes the geographic detector to analyze the driving factors of CO_2 emissions from future expansion land. The parameters used in the analysis are economic and population variables, without considering other potential drivers.

A variety of factors contribute to the spatial distribution of CO_2 emissions, but the study recognizes that its consideration of these factors is still not complete. Future research could broaden CO_2 emission predictions to include industrial and rural areas. Additionally, integrating more types of data related to CO_2 emissions, such as factory distribution, building density, and population mobility data, into the model could reduce the uncertainty of the predictive model and more accurately forecast the spatial distribution of future CO_2 emissions. Moreover, CO_2 emissions may also be related to a multitude of other factors, such as urban policies and cultural differences; for instance, the population structure and socio-economic scale can influence CO_2 emissions [67]. Future studies should incorporate these factors into the model to enhance its explanatory power and predictive accuracy. Different societal scenarios lead to diverse trajectories of urban economic development, resulting in variations in the urban population, economic growth, industrial structure, and other factors, which could impact future projections of urban land CO_2 emissions [68,69]. To enhance the model's applicability, the future development trends of urban CO_2 emissions

could be segmented into multiple grades. When training the model, correction parameters or modules for the total urban CO_2 emissions should be added to train CO_2 emission forecasting models under a variety of societal scenarios. Additionally, classifying cities by their morphology and function can improve the model's precision and extend its application to a wider range. Furthermore, utilizing urban spatial form and ecological levels can provide an in-depth analysis of the potential factors driving CO_2 emissions from expanding urban land [70].

5. Conclusions

This study proposed an innovative spatial prediction model for urban land CO_2 emissions, utilizing data on socioeconomic grids, land utilization, and CO_2 emissions. Furthermore, based on socioeconomic grid data, such as NTL and POP, the model predicted the spatial distribution of urban land CO_2 emissions in the study area for 2030. Additionally, factors affecting the increase in CO_2 emissions and the decrease in carbon sequestration due to future urban expansion were analyzed using the geographical detector. Overall, by analyzing cities in the upper, middle, and lower reaches, the study offers suggestions for decreasing CO_2 emissions in urban areas.

The results show that the CO_2 emission spatial prediction model established in this study achieved an R-squared of 0.73 in the YREB, effectively predicting urban land CO_2 emissions. From 2005 to 2030, CO_2 emissions are on the rise, with cities, such as Nanjing and Shanghai, expected to experience substantial increases, while Wuhan and Changsha will see slower growth. Guizhou's emissions gradually decline after 2015 due to a decrease in the population density. Additionally, the combined effect of TI, BR, and PD drives the increase in CO_2 emissions from urban land expansion and also influences the decrease in carbon sequestration from urban land expansion, though to a lesser extent. CO_2 emissions in downstream cities are influenced by population and economic development, while those in midstream city clusters are mainly driven by economic development. In upstream city clusters, CO_2 emissions are primarily driven by economic development, but an investment in science and technology helps to mitigate them.

Based on our results, different developing directions and routes can be implemented in the YERB: (1) downstream city clusters with rapid urban expansion and high CO_2 emissions require urgent attention. Cities should limit population density, control urban land expansion, and promote energy conservation and low-carbon transportation to reduce CO_2 emissions. (2) In midstream city clusters, stable CO_2 emission growth is driven by economic development and land expansion. It is important to transition to low-carbon energy sources to achieve early carbon peaking in future development. (3) Increased investment in science and technology can help reduce CO_2 emissions in upstream city clusters. Future efforts should focus on boosting such investments while monitoring urban expansion in specific cities.

Author Contributions: C.W.: Conceptualization, Formal analysis, Methodology, Visualization, Writing—review and editing. J.W.: Formal analysis, Writing—original draft, Writing—review and editing. L.M.: Conceptualization, Writing—review and editing. M.J.: Writing—review and editing. J.C.: Writing—review and editing. Z.S.: Funding acquisition, Supervision. N.C.: Supervision, Writing—review and editing. All authors have read and agreed to the published version of the manuscript.

Funding: This research was funded by the National Key Research and Development Program of China (No. 2023YFC3209101), the Key R&D Program of Hubei Province (No. 2022BAA048), the National Nature Science Foundation of China Program (No. 42371101), the CRSRI Open Research Program (Program SN: CKWV20231198/KY), and the Open Fund of National Engineering Research Center for Geographic Information System, China University of Geosciences, (Grant No. 2022KFJJ07).

Data Availability Statement: Data are contained within the article.

Acknowledgments: The numerical calculations in this paper have been performed on the supercomputing system in the Supercomputing Center of Wuhan University.

Conflicts of Interest: The authors declare that they have no known competing financial interests or personal relationships that could have appeared to influence the work reported in this paper.

References

1. Ma, L.; Xiang, L.; Wang, C.; Chen, N.; Wang, W. Spatiotemporal evolution of urban carbon balance and its response to new-type urbanization: A case of the middle reaches of the Yangtze River Urban Agglomerations, China. *J. Clean. Prod.* **2022**, *380*, 135122. [CrossRef]
2. Yuan, X.; Wang, C.; Li, B.; Wang, W.; Chen, N. Review of the Driving Forces and Impacts of Land Use/Cover Change in the Yangtze River Basin. *Geomat. Inf. Sci. Wuhan Univ.* **2023**, *48*, 1241–1255. [CrossRef]
3. Zhang, Z.; Pan, S.-Y.; Li, H.; Cai, J.; Olabi, A.G.; Anthony, E.J.; Manovic, V. Recent advances in carbon dioxide utilization. *Renew. Sustain. Energy Rev.* **2020**, *125*, 109799. [CrossRef]
4. UN-Habitat. *World Cities Report 2022: Envisaging the Future of Cities*; UN-Habitat: Nairobi, Kenya, 2022; pp. 41–44.
5. Zhao, P.; Zhang, M. The impact of urbanisation on energy consumption: A 30-year review in China. *Urban Clim.* **2018**, *24*, 940–953. [CrossRef]
6. Kennedy, C.; Steinberger, J.; Gasson, B.; Hansen, Y.; Hillman, T.; Havránek, M.; Pataki, D.; Phdungsilp, A.; Ramaswami, A.; Mendez, G.V. Methodology for inventorying greenhouse gas emissions from global cities. *Energy Policy* **2010**, *38*, 4828–4837. [CrossRef]
7. Al-Mulali, U.; Binti Che Sab, C.N.; Fereidouni, H.G. Exploring the bi-directional long run relationship between urbanization, energy consumption, and carbon dioxide emission. *Energy* **2012**, *46*, 156–167. [CrossRef]
8. Wang, C.; Jia, M.; Chen, N.; Wang, W. Long-Term Surface Water Dynamics Analysis Based on Landsat Imagery and the Google Earth Engine Platform: A Case Study in the Middle Yangtze River Basin. *Remote Sens.* **2018**, *10*, 1635. [CrossRef]
9. Liu, X.; Wang, S.; Wu, P.; Feng, K.; Hubacek, K.; Li, X.; Sun, L. Impacts of Urban Expansion on Terrestrial Carbon Storage in China. *Environ. Sci. Technol.* **2019**, *53*, 6834–6844. [CrossRef]
10. Zhang, D.; Wang, Z.; Li, S.; Zhang, H. Impact of Land Urbanization on Carbon Emissions in Urban Agglomerations of the Middle Reaches of the Yangtze River. *Int. J. Environ. Res. Public Health* **2021**, *18*, 1403. [CrossRef]
11. Huang, S.; Gan, Y.; Chen, N.; Wang, C.; Zhang, X.; Li, C.; Horton, D.E. Urbanization enhances channel and surface runoff: A quantitative analysis using both physical and empirical models over the Yangtze River basin. *J. Hydrol.* **2024**, *635*, 131194. [CrossRef]
12. Huang, S.; Gan, Y.; Zhang, X.; Chen, N.; Wang, C.; Gu, X.; Ma, J.; Niyogi, D. Urbanization Amplified Asymmetrical Changes of Rainfall and Exacerbated Drought: Analysis over Five Urban Agglomerations in the Yangtze River Basin, China. *Earths Future* **2023**, *11*, e2022EF003117. [CrossRef]
13. Luqman, M.; Rayner, P.J.; Gurney, K.R. On the impact of urbanisation on CO_2 emissions. *NPJ Urban Sustain.* **2023**, *3*, 6. [CrossRef]
14. Wang, J.; Cai, B.; Zhang, L.; Cao, D.; Liu, L.; Zhou, Y.; Zhang, Z.; Xue, W. High Resolution Carbon Dioxide Emission Gridded Data for China Derived from Point Sources. *Environ. Sci. Technol.* **2014**, *48*, 7085–7093. [CrossRef]
15. Ma, L.; Wang, C.; Xiang, L.; Liu, J.; Dang, C.; Wu, H. Chinese cities show different trend toward carbon peak. *Sci. Total Environ.* **2024**, *934*, 173156. [CrossRef] [PubMed]
16. Zhang, Y.; Quan, J.; Kong, Y.; Wang, Q.; Zhang, Y.; Zhang, Y. Research on the fine-scale spatial-temporal evolution characteristics of carbon emissions based on nighttime light data: A case study of Xi'an city. *Ecol. Inf.* **2024**, *79*, 102454. [CrossRef]
17. Wang, G.; Hu, Q.; He, L.; Guo, J.; Huang, J.; Zhong, L. The estimation of building carbon emission using nighttime light images: A comparative study at various spatial scales. *Sustain. Cities Soc.* **2024**, *101*, 105066. [CrossRef]
18. Chuai, X.; Feng, J. High resolution carbon emissions simulation and spatial heterogeneity analysis based on big data in Nanjing City, China. *Sci. Total Environ.* **2019**, *686*, 828–837. [CrossRef]
19. Bai, D.; Dong, Q.; Khan, S.A.R.; Li, J.; Wang, D.; Chen, Y.; Wu, J. Spatio-temporal heterogeneity of logistics CO_2 emissions and their influencing factors in China: An analysis based on spatial error model and geographically and temporally weighted regression model. *Environ. Technol. Innov.* **2022**, *28*, 102791. [CrossRef]
20. Cai, M.; Shi, Y.; Ren, C. Developing a high-resolution emission inventory tool for low-carbon city management using hybrid method—A pilot test in high-density Hong Kong. *Energy Build.* **2020**, *226*, 110376. [CrossRef]
21. Gao, F.; Wu, J.; Xiao, J.; Li, X.; Liao, S.; Chen, W. Spatially explicit carbon emissions by remote sensing and social sensing. *Environ. Res.* **2023**, *221*, 115257. [CrossRef] [PubMed]
22. Zhou, Y.; Chen, M.; Tang, Z.; Mei, Z. Urbanization, land use change, and carbon emissions: Quantitative assessments for city-level carbon emissions in Beijing-Tianjin-Hebei region. *Sustain. Cities Soc.* **2021**, *66*, 102701. [CrossRef]
23. Guo, B.; Xie, T.; Zhang, W.; Wu, H.; Zhang, D.; Zhu, X.; Ma, X.; Wu, M.; Luo, P. Rasterizing CO_2 emissions and characterizing their trends via an enhanced population-light index at multiple scales in China during 2013–2019. *Sci. Total Environ.* **2023**, *905*, 167309. [CrossRef] [PubMed]
24. Meng, X.; Han, J.; Huang, C. An Improved Vegetation Adjusted Nighttime Light Urban Index and Its Application in Quantifying Spatiotemporal Dynamics of Carbon Emissions in China. *Remote Sens.* **2017**, *9*, 829. [CrossRef]
25. Guo, W.; Li, Y.; Li, P.; Zhao, X.; Zhang, J. Using a combination of nighttime light and MODIS data to estimate spatiotemporal patterns of CO_2 emissions at multiple scales. *Sci. Total Environ.* **2022**, *848*, 157630. [CrossRef] [PubMed]

26. Sun, J.; Qi, Y.; Guo, J.; Zheng, J.; Zhang, L.; Yang, X. Impact of nighttime light data saturation correction on the application of carbon emissions spatialization: A comparative study of the correction effect and application effect based on five methods in China. *J. Clean. Prod.* **2024**, *438*, 140815. [CrossRef]
27. Tao, L.; Su, Y.; Fang, X. Global carbon emission spatial pattern in 2030 under INDCs: Using a gridding approach based on population and urbanization. *Int. J. Clim. Change Strateg. Manag.* **2021**, *14*, 78–99. [CrossRef]
28. Luo, H.; Li, Y.; Gao, X.; Meng, X.; Yang, X.; Yan, J. Carbon emission prediction model of prefecture-level administrative region: A land-use-based case study of Xi'an city, China. *Appl. Energy* **2023**, *348*, 121488. [CrossRef]
29. Huang, Y.; Shen, L.; Liu, H. Grey relational analysis, principal component analysis and forecasting of carbon emissions based on long short-term memory in China. *J. Clean. Prod.* **2019**, *209*, 415–423. [CrossRef]
30. Meng, L.; Graus, W.; Worrell, E.; Huang, B. Estimating CO_2 (carbon dioxide) emissions at urban scales by DMSP/OLS (Defense Meteorological Satellite Program's Operational Linescan System) nighttime light imagery: Methodological challenges and a case study for China. *Energy* **2014**, *71*, 468–478. [CrossRef]
31. Yang, D.; Luan, W.; Qiao, L.; Pratama, M. Modeling and spatio-temporal analysis of city-level carbon emissions based on nighttime light satellite imagery. *Appl. Energy* **2020**, *268*, 114696. [CrossRef]
32. Wei, W.; Zhang, X.; Zhou, L.; Xie, B.; Zhou, J.; Li, C. How does spatiotemporal variations and impact factors in CO_2 emissions differ across cities in China? Investigation on grid scale and geographic detection method. *J. Clean. Prod.* **2021**, *321*, 128933. [CrossRef]
33. Wen, J.; Chuai, X.; Li, S.; Song, S.; Li, Y.; Wang, M.; Wu, S. Spatial Heterogeneity of the Carbon Emission Effect Resulting from Urban Expansion among Three Coastal Agglomerations in China. *Sustainability* **2019**, *11*, 4590. [CrossRef]
34. Liu, G.; Zhang, F. How do trade-offs between urban expansion and ecological construction influence CO_2 emissions? New evidence from China. *Ecol. Indic.* **2022**, *141*, 109070. [CrossRef]
35. Wang, S.; Fang, C.; Wang, Y.; Huang, Y.; Ma, H. Quantifying the relationship between urban development intensity and carbon dioxide emissions using a panel data analysis. *Ecol. Indic.* **2015**, *49*, 121–131. [CrossRef]
36. Ke, N.; Lu, X.; Zhang, X.; Kuang, B.; Zhang, Y. Urban land use carbon emission intensity in China under the "double carbon" targets: Spatiotemporal patterns and evolution trend. *Environ. Sci. Pollut. Res.* **2023**, *30*, 18213–18226. [CrossRef]
37. Wen, F.; Yang, S.; Huang, D. Heterogeneous human capital, spatial spillovers and regional innovation: Evidence from the Yangtze River Economic Belt, China. *Humanit. Soc. Sci. Commun.* **2023**, *10*, 365. [CrossRef]
38. Yang, J.; Li, Z.; Zhang, D.; Yu, K.; Zhong, J.; Zhu, J. Spatial distribution characteristics and variability of urban ecological welfare performance in the Yangtze River economic Belt: Evidence from 70 cities. *Ecol. Indic.* **2024**, *160*, 111846. [CrossRef]
39. Yu, X.; Wu, Z.; Zheng, H.; Li, M.; Tan, T. How urban agglomeration improve the emission efficiency? A spatial econometric analysis of the Yangtze River Delta urban agglomeration in China. *J. Environ. Manag.* **2020**, *260*, 110061. [CrossRef]
40. Zhang, Z.; Jin, G. Spatiotemporal differentiation of carbon budget and balance zoning: Insights from the middle reaches of the Yangtze River Urban Agglomeration, China. *Appl. Geogr.* **2024**, *167*, 103293. [CrossRef]
41. Wei, W.; Wang, N.; Yin, L.; Guo, S.; Bo, L. Spatio-temporal evolution characteristics and driving mechanisms of Urban–Agricultural–Ecological space in ecologically fragile areas: A case study of the upper reaches of the Yangtze River Economic Belt, China. *Land Use Policy* **2024**, *145*, 107282. [CrossRef]
42. Zhou, R. Economic growth, energy consumption and CO_2 emissions—An empirical study based on the Yangtze River economic belt of China. *Heliyon* **2023**, *9*, e19865. [CrossRef]
43. Zhang, S.; Kharrazi, A.; Yu, Y.; Ren, H.; Hong, L.; Ma, T. What causes spatial carbon inequality? Evidence from China's Yangtze River economic Belt. *Ecol. Indic.* **2021**, *121*, 107129. [CrossRef]
44. Ji, R.; Wang, C.; Wang, W.; Liao, S.; Chen, N. Spatiotemporal evolution of carbon balance based on the enhanced two-step floating catchment area (E2SFCA) method in the Yangtze River Economic Belt, China. *Environ. Dev. Sustain.* **2024**, *26*, 8979–9004. [CrossRef]
45. Ding, X.; Tang, N.; He, J. The Threshold Effect of Environmental Regulation, FDI Agglomeration, and Water Utilization Efficiency under "Double Control Actions"—An Empirical Test Based on Yangtze River Economic Belt. *Water* **2019**, *11*, 452. [CrossRef]
46. Chen, J.; Gao, M. Global 1 km × 1 km gridded revised real gross domestic product and electricity consumption during 1992–2019 based on calibrated nighttime light data. *Figshare Dataset* **2021**. [CrossRef]
47. Chen, G.; Li, X.; Liu, X.; Chen, Y.; Liang, X.; Leng, J.; Xu, X.; Liao, W.; Qiu, Y.; Wu, Q.; et al. A global urban land expansion product at 1-km resolution for 2015 to 2100 based on the SSP scenarios. *PANGAEA* **2019**. [CrossRef]
48. Hochreiter, S.; Schmidhuber, J. Long Short-Term Memory. *Neural Comput.* **1997**, *9*, 1735–1780. [CrossRef]
49. Fan, Z.; Duan, J.; Lu, Y.; Zou, W.; Lan, W. A geographical detector study on factors influencing urban park use in Nanjing, China. *Urban For. Urban Green.* **2021**, *59*, 126996. [CrossRef]
50. Zhang, J.; Zhang, P.; Gu, X.; Deng, M.; Lai, X.; Long, A.; Deng, X. Analysis of Spatio-Temporal Pattern Changes and Driving Forces of Xinjiang Plain Oases Based on Geodetector. *Land* **2023**, *12*, 1508. [CrossRef]
51. Wang, J.; Li, X.; Christakos, G.; Liao, Y.; Zhang, T.; Gu, X.; Zheng, X. Geographical Detectors-Based Health Risk Assessment and its Application in the Neural Tube Defects Study of the Heshun Region, China. *Int. J. Geogr. Inf. Sci.* **2010**, *24*, 107–127. [CrossRef]
52. Wang, J.; Zhang, T.; Fu, B. A measure of spatial stratified heterogeneity. *Ecol. Indic.* **2016**, *67*, 250–256. [CrossRef]
53. Chen, B.; Wu, C.; Huang, X.; Yang, X. Examining the Relationship between Urban Land Expansion and Economic Linkage Using Coupling Analysis: A Case Study of the Yangtze River Economic Belt, China. *Sustainability* **2020**, *12*, 1227. [CrossRef]

54. Sun, C.; Wang, B.; Miao, H. Spatiotemporal dynamics of CO_2 emissions: A case study of the "New Yangtze River Delta" in China. *Environ. Sci. Pollut. Res.* **2023**, *30*, 40961–40977. [CrossRef]
55. Xu, L.; Chen, N.; Chen, Z.; Zhang, C.; Yu, H. Spatiotemporal forecasting in earth system science: Methods, uncertainties, predictability and future directions. *Earth Sci. Rev.* **2021**, *222*, 103828. [CrossRef]
56. Yu, T.; Liu, C.; Li, W.; Huang, W.; Wu, H.; Fan, Z. Characterizing urban actively populated area growth in the Yangtze River Delta using nighttime light data. *Int. J. Appl. Earth Obs. Geoinf.* **2024**, *129*, 103857. [CrossRef]
57. Zhu, L.; Li, Z.; Yang, X.; Zhang, Y.; Li, H. Forecast of Transportation CO_2 Emissions in Shanghai under Multiple Scenarios. *Sustainability* **2022**, *14*, 13650. [CrossRef]
58. Ma, Z.; Duan, X.; Wang, L.; Wang, Y.; Kang, J.; Yun, R. A Scenario Simulation Study on the Impact of Urban Expansion on Terrestrial Carbon Storage in the Yangtze River Delta, China. *Land* **2023**, *12*, 297. [CrossRef]
59. Yuan, Y.; Suk, S. Decomposition Analysis and Trend Prediction of Energy-Consumption CO_2 Emissions in China's Yangtze River Delta Region. *Energies* **2023**, *16*, 4510. [CrossRef]
60. Luo, H.; Wang, C.; Li, C.; Meng, X.; Yang, X.; Tan, Q. Multi-scale carbon emission characterization and prediction based on land use and interpretable machine learning model: A case study of the Yangtze River Delta Region, China. *Appl. Energy* **2024**, *360*, 122819. [CrossRef]
61. Hu, J.; Shao, C.; Zhang, Z. The Impact of Sustainable Regional Development Policy on Carbon Emissions: Evidence from Yangtze River Delta of China. *Energies* **2022**, *15*, 9492. [CrossRef]
62. Wu, S.; Hu, S.; Frazier, A.E.; Hu, Z. China's urban and rural residential carbon emissions: Past and future scenarios. *Resour. Conserv. Recycl.* **2023**, *190*, 106802. [CrossRef]
63. Yu, T.; Shu, T.; Xu, J. Spatial pattern, and evolution of China's urban agglomerations. *Front. Urban Rural Plan.* **2024**, *2*, 7. [CrossRef]
64. Pu, X.; Liu, H.; Peng, X. Spatial-Temporal Evolution of Green Development Efficiency of Urban Agglomeration in the Upper Reaches of the Yangtze River. *Pol. J. Environ. Stud.* **2022**, *31*, 5207–5219. [CrossRef]
65. Wang, W.; Yu, H.; Tong, X.; Jia, Q. Estimating terrestrial ecosystem carbon storage change in the YREB caused by land-use change under SSP-RCPs scenarios. *J. Clean. Prod.* **2024**, *469*, 143205. [CrossRef]
66. Chuai, X.; Xia, M.; Xiang, A.; Miao, L.; Zhao, R.; Zuo, T. Vegetation coverage and carbon sequestration changes in China's forest projects area. *Glob. Ecol. Conserv.* **2022**, *38*, e02257. [CrossRef]
67. Wang, G.; Feng, Y. Analysis of carbon emission drivers and peak carbon forecasts for island economies. *Ecol. Modell.* **2024**, *489*, 110611. [CrossRef]
68. Li, X.; Lin, C.; Lin, M.; Jim, C.Y. Drivers, scenario prediction and policy simulation of the carbon emission system in Fujian Province (China). *J. Clean. Prod.* **2024**, *434*, 140375. [CrossRef]
69. Gao, X.; Zhao, M.; Zhang, M.; Guo, Z.; Liu, X.; Yuan, Z. Carbon conduction effect and multi-scenario carbon emission responses of land use patterns transfer: A case study of the Baiyangdian basin in China. *Front. Environ. Sci.* **2024**, *12*, 1374383. [CrossRef]
70. Guo, Y.; Zhang, Z. Reducing carbon emissions through green renewal: Insights from residential energy consumption in Chinese urban inventory districts from an evidence-based decision-making perspective. *Humanit. Soc. Sci. Commun.* **2024**, *11*, 54. [CrossRef]